International Journal of Pharmaceutics 432 (2012) 32–41

Contents lists available at SciVerse ScienceDirect

International Journal of Pharmaceutics

journal homepage: www.elsevier.com/locate/ijpharm

Effect of expansion chamber geometry on atomization and spray dispersion characters of a flashing mixture containing inerts. Part II: High speed imaging measurements

Dehao Ju[a], John Shrimpton[a,*], Moira Bowdrey[b], Alex Hearn[b]

[a] Energy Technology Group, School of Engineering Sciences, Highfield Campus, University of Southampton, Southampton SO17 1BJ, UK
[b] Kind Consumer Limited, London, UK

ARTICLE INFO

Article history:
Received 28 October 2011
Received in revised form 22 April 2012
Accepted 23 April 2012
Available online 3 May 2012

Keywords:
Nicotine
Smoking
Metered dose inhalers
Breath activation

ABSTRACT

A breath activated, pressurized metered dose inhaler (pMDI) device (Oxette®) has been developed to replace the traditional cigarette. In this paper, internal and external spray characters are measured by high speed imaging along with sizing the residual droplets at the distance from the discharge orifice where the human oropharynx locates. Two different formulations with 95% and 98% mass fraction of HFA 134a and two prototype cigarette alternatives with different expansion chamber volumes have been analyzed. The internal and external flows issuing from early stage prototype Oxette® are discussed along with boiling and evaporation phenomena. The expansion and entrainment regions of the jet are observed and discussed with comparison to the turbulent round jet of a single phase. From the visualizations of internal flows in the earlier design, a small expansion chamber can hardly generate small bubbles, which is difficult to produce fine sprays. The larger the expansion chamber volume, the more room for the propellant evaporation, recirculation, bubble generation and growth, all of which produces finer sprays. Therefore the later prototype of Oxette® 2 made a significant improvement to produce fine sprays and facilitated development of the cigarette alternative. Furthermore, the characters of the spray generated by Oxette® are compared to that issuing from a pMDI by previous researchers, where the residual MMD is larger than that of a pMDI, because the Oxette® has a smaller expansion chamber and the geometry provides less opportunity for the recirculation due to restrictions of the design space. Although the formulation with higher mass fraction of HFA 134a can generate smaller droplets, it cannot produce steady puffs with relatively low mass flow rate.

© 2012 Elsevier B.V. All rights reserved.

1. Introduction

In a pharmaceutical pressurized metered dose inhaler (pMDI), a mixture of propellant and physically but biologically active inert is actuated by means of a twin-orifice system. The effectiveness of such a system in producing finely atomized sprays has been known since the start of the 20th century. The principle has been used in pharmaceutical applications since Riker Laboratories developed the first metered dose inhaler (pMDI) in the late 1950s (Versteeg et al., 2006). Subsequently, the pressurized metered dose inhaler (pMDI) has become the most prescribed drug delivery system for treating respiratory diseases. The compactness, ease of use, low cost of these devices and reasonable effectiveness in treating lung diseases has ensured strong preference amongst patients as well as clinicians.

Kind Consumer Ltd. intends to use the same concept design to pMDIs to deliver a nicotine based formulation to mimic smoking, and use breath activation to achieve good actuation/inhalation coordination. The pMDI-like devices have some well-known limitations, the most important being their low drug delivery efficiency which is between 5% and 20% (Versteeg et al., 2006). The conventional pMDIs are known to produce aerosol with excessively high velocities and a substantial fraction of large droplets, which causes high oropharyngeal deposition. Poor coordination between pMDI actuation and inhalation by many patients compounds the problem. Apart from reducing the dose available for delivering to the lungs, this unintended deposition in the oropharynx often causes oral thrush and in about 5% patients, cough and bronchospasm (Versteeg et al., 2006). Therefore a detailed research on the spray characteristics is required.

Due to the absence of suitable instrumentation, few visualizations of the two-phase flow associated with pre-atomization inside the expansion chamber of the twin-orifice system and the subsequent external spray formation have been provided. Dunbar (1996)

* Corresponding author.
E-mail address: John.Shrimpton@soton.ac.uk (J. Shrimpton).

0378-5173/$ – see front matter © 2012 Elsevier B.V. All rights reserved.
http://dx.doi.org/10.1016/j.ijpharm.2012.04.064

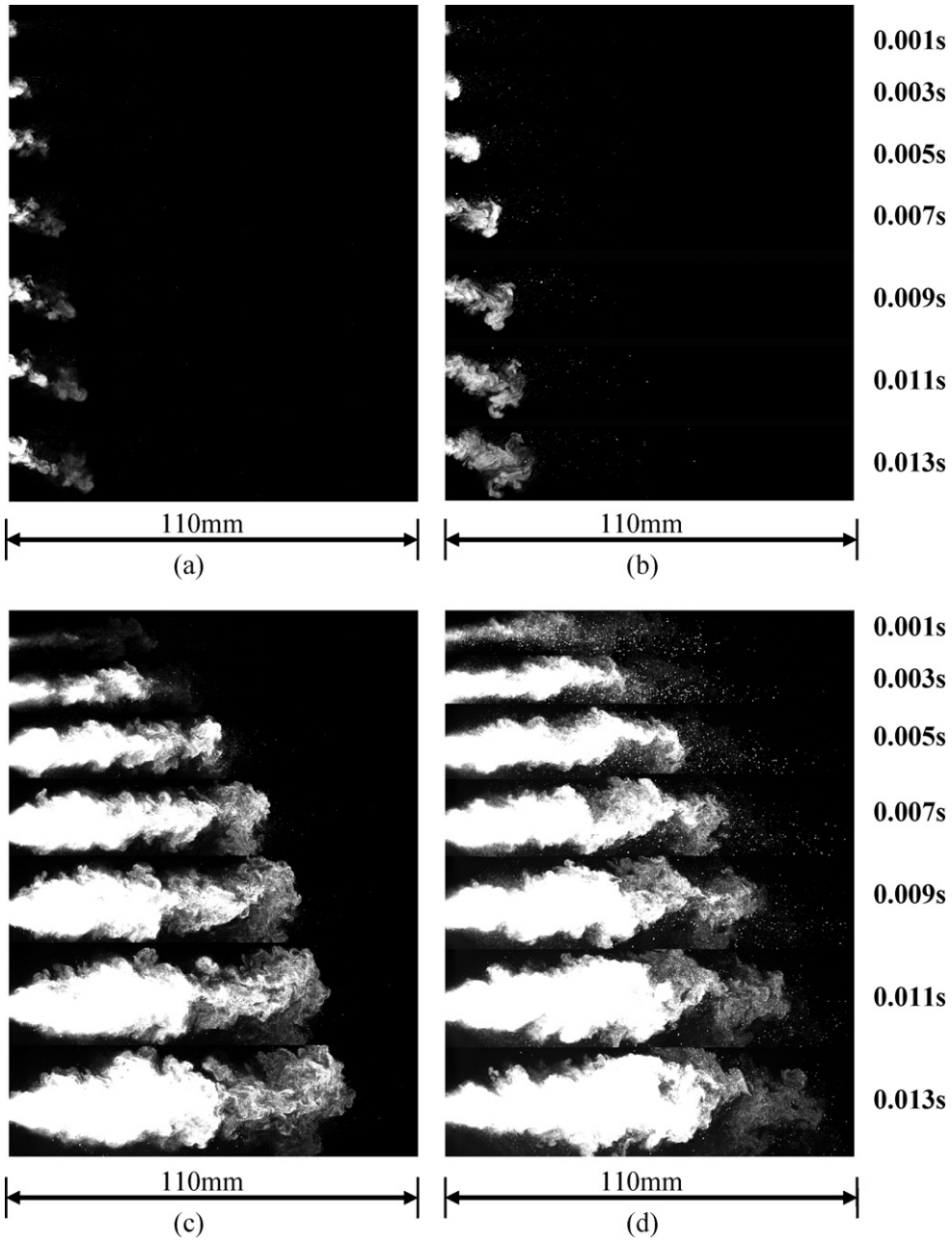

Fig. 1. Spray visualizations during 0.001–0.013 s after the start of the 1st shallow inhalation: (a) with Oxette® 1 for the Formulation 1 (95% HFA 134a); (b) with Oxette® 1 for Formulation 2 (98% HFA 134a); (c) with Oxette® 2 for the Formulation 1 (95% HFA 134a); and (d) with Oxette® 2 for Formulation 2 (98% HFA 134a). Oxette® 2 performed much better than Oxette® 1.

presented small selections of high-speed photographs, but it is difficult to obtain a clear picture of flow conditions. Versteeg et al. (2006) investigated the propellant flow inside the expansion chamber of a pMDI by high speed imaging. They found the existence of an annular flow regime with a vapour core and an unsteady wall film consisting of foamy liquid in the expansion chamber. Vu and Aguilar (2009) studied a flashing jet with superheated water by high speed visualization of the internal nozzle flow. They found that the clear bubbles formed near the nozzle wall and an annular flow existed in which the bubbles merged into a vapour core surrounded by a liquid sheath.

In spite of its therapeutic significance the spray generation mechanism of the pMDI has not been extensively researched. External spray characteristics in the far-field (x = 0–100 mm) were documented in two studies by (i) Clark (1991) with an aerodynamic particle sizer and (ii) Dunbar (1996) by means of Phase Doppler Anemometry (PDA).

In the present study, two prototypes of 'cigarettes' (named here as Oxette®) with different expansion chamber volumes were investigated, a schematic diagram is shown in Fig. 1 in Ju et al. (2012). Using high speed imaging, spray characters and drop sizes were studied at sequential puffs under different smoking patterns which is illustrated in Fig. 2 of Ju et al. (2012). This work will be useful for future researchers investigating flash evaporation systems including the internal and external flows since it informs on the effect of both geometrical and formulation changes, including presence of inerts on the final spray quality, and provides verification of a model used to predict such changes.

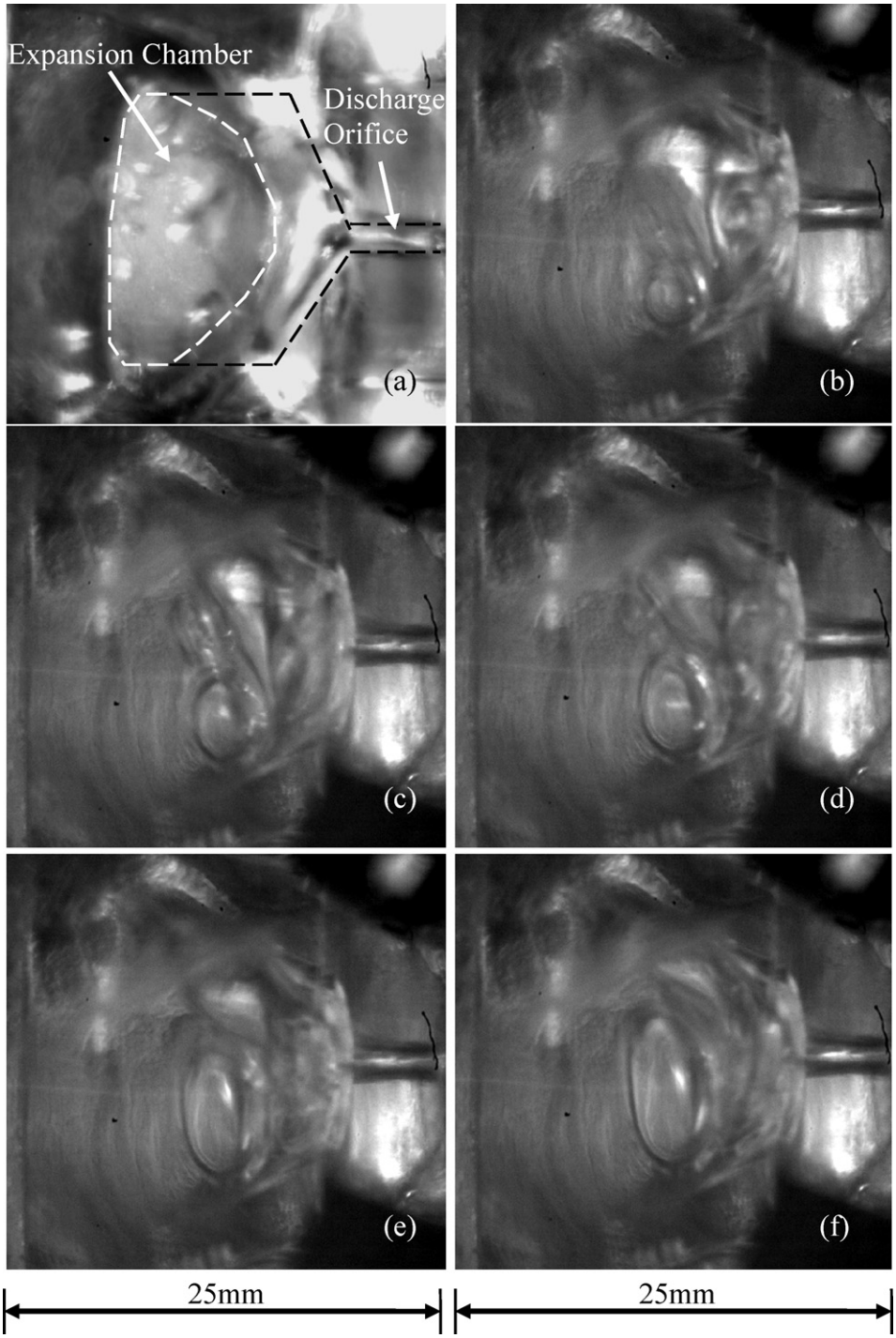

Fig. 2. Visualization of internal flow regime inside expansion chamber of Oxette® 1: (a) presents the cross-section of the expansion chamber and the discharge orifice without any flows; (b)–(f) sequential images of the bubble growth in the expansion chamber within 0.008 s recorded at 500 Hz.

2. Experimental procedure

Two prototypes of the cigarette alternatives, named here as Oxette® 1 for the earlier design and Oxette® 2 for the later design, were manufactured at early stage by Kind Consumer Ltd., as introduced in Ju et al. (2012). The same dimensions of the two devices are the metering chamber volume of 600 mm^3, the discharge orifice diameter (d_e) of 0.2 mm and the expansion chamber diameter (D_{EC}) of 1.0 mm. The inlet orifice diameters (d_i) change between 0.14 mm and 0.18 mm due to the inhaled pressure variation, and a mean value of 0.17 mm is used in the simulation. The expansion chamber lengths (L_{EC}) of Oxette® 1 and Oxette® 2 are 2.0 mm and 6.9 mm respectively. Sprays actuated from the Oxette® were imaged using laser-based high-speed visualization to reveal internal propellant flows and external sprays. The system comprised a Nd-YLF (yttrium lithium fluoride) laser (Darwin-Duo-527-40-M) as the illumination source in conjunction with a Fastcam SA1.1 high-speed digital camera for image recording. The laser provided a pulsed light source with a frequency of 0.1–10 kHz. The camera provided 1024 × 1024 pixel resolution images and was operated with a SIGMA (105 mm, F/2.8) lens to image the expansion chamber, near-orifice region and the global spray development. A Questar QM100 lens was used to

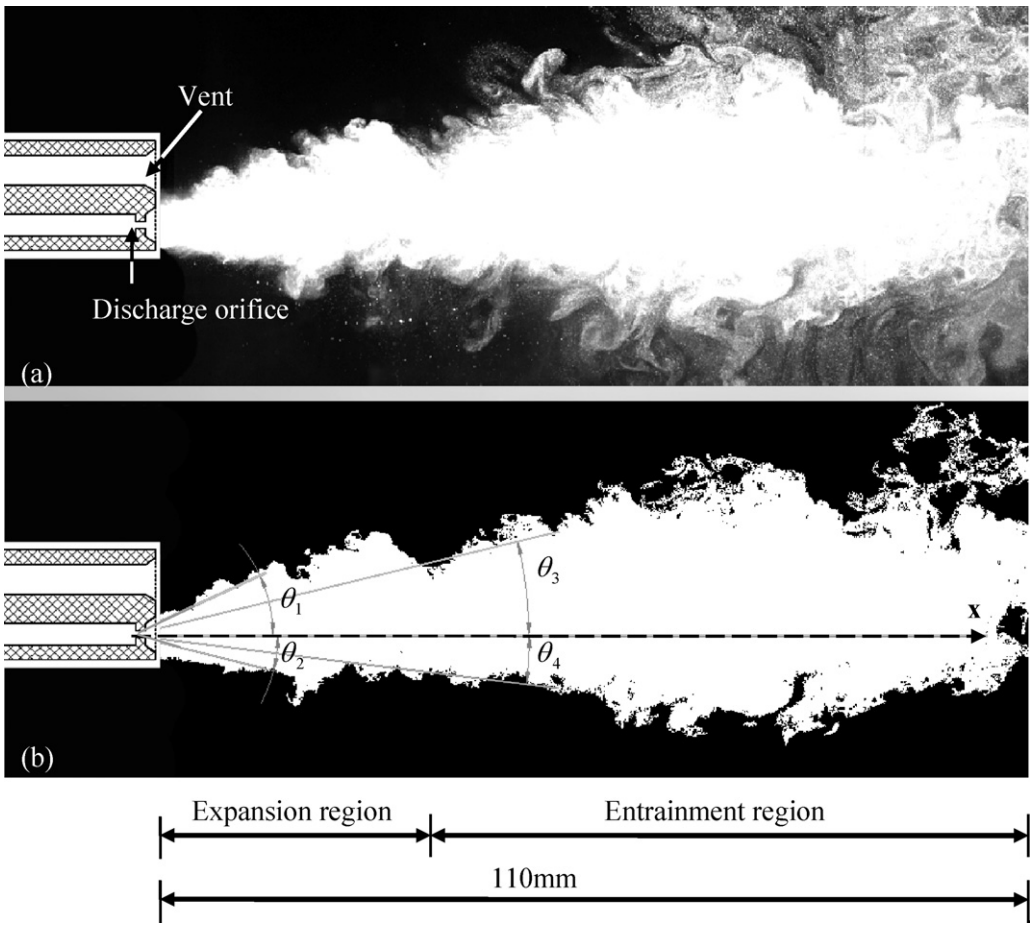

Fig. 3. A sample of jet generated under 1st shallow inhalation with Oxette® 2 for the Formulation 1 (95% HFA 134a) (a) the original image and (b) the image after process with a threshold level of 85% of the background intensity (θ_1 and θ_2 are the half spray angles in the expansion region; θ_3 and θ_4 are the half spray angles of the entire spray).

size the droplets at the axial position of 100 mm from the discharge orifice at much higher magnification. Formulation 1 with 95% mass fraction of propellant and Formulation 2 with 98% mass fraction of propellant were analyzed and the Oxette® was actuated by the mechanical lung (Ju et al., 2010) under shallow and deep smoking profiles (Ju et al., 2012). The physical properties of the propellant are listed in the previous publication (Ju et al., 2010).

3. Results

3.1. Internal and external spray characters

Fig. 1(a) and (b) shows the spray development at the start (0.001–0.013 s) of the actuation flow under the 1st shallow inhalation for the Formulation 1 (95% HFA 134a) and Formulation 2

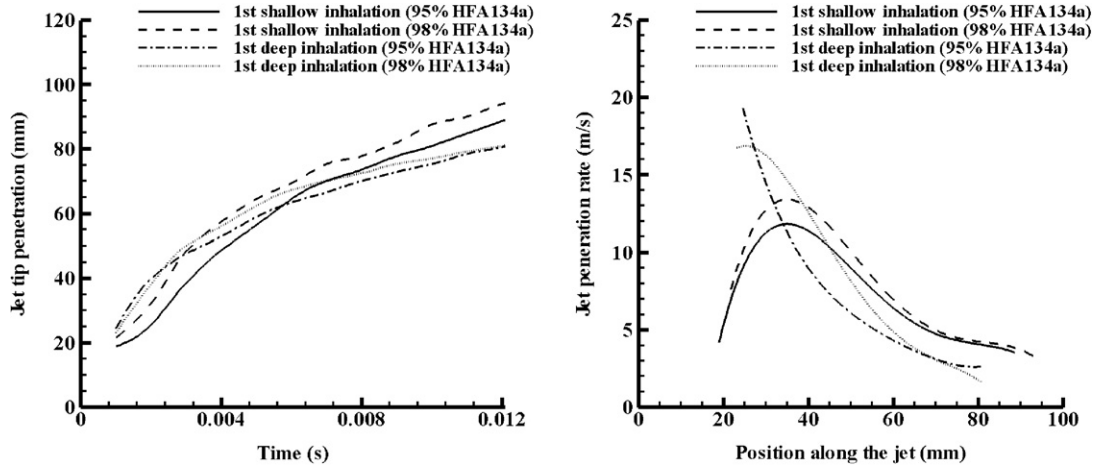

Fig. 4. Left: The corresponding jet tip penetration at each time step from 0.001 s to 0.012 s under 1st shallow inhalation profile for the Formulation 1 (95% HFA 134a) and Formulation 2 (98% HFA 134a). Right: Jet penetration rate along the jet during the first 0.001–0.012 s.

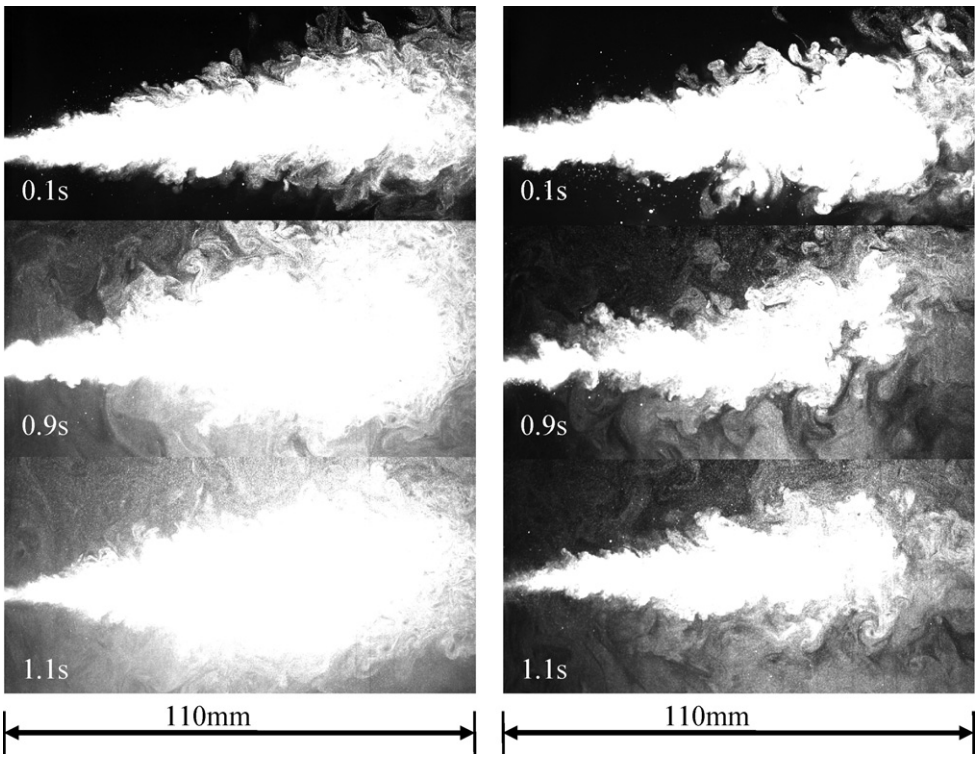

Fig. 5. Left: Spray visualization from 0.1 s to 1.1 s under 1st shallow inhalation with Oxette® 2 for the Formulation 1 (95% HFA 134a). Right: Spray visualization from 0.1 s to 1.1 s under 1st shallow inhalation with Oxette® 2 for the Formulation 2 (98% HFA 134a). Formulation 1 produced a denser spray than Formulation 2.

(98% HFA 134a) by Oxette® 1. It shows Oxette® 1 cannot produce fully developed fine sprays, which indicates the small expansion chamber cannot provide enough space and time for the bubble nucleation and formation to generate aerosols. However, Formulation 2 (98% HFA 134a) generated a more "violent" spray (notable boiling phenomena) compared to Formulation 1 (95% HFA 134a), due to its higher mass fraction of volatile propellant (HFA 134a). Fig. 2 provides sequential visualizations of internal flow regime inside expansion chamber of Oxette® 1 during the actuation at a 500 Hz frame rate. Fig. 2a presents the cross section of the expansion chamber and the discharge orifice without any flow. A bubble began to form at the bottom of the expansion chamber (Fig. 2b), and grew/expanded during the next 0.008 s as shown in Fig. 2c–f, meanwhile it pushed the liquid out through the discharge orifice. Oxette® 1 provides only a small expansion chamber volume to form small bubbles but squeezes them into a large single bubble, which causes it to function as a plain-orifice atomizer resulting in poor atomization. Since Oxette® 1 produces a poor spray, we will not discuss its spray characteristics in the following sections, however the companion paper (Ju et al., 2012) provides general spray plume characteristics.

Fig. 1(c) and (d) shows the spray development at the start (0.001–0.013 s) of the actuation flow under the 1st shallow inhalation for Formulation 1 and Formulation 2 by Oxette® 2. Flashing is shown to be occurring outside the discharge orifice but it may begin inside the discharge orifice or expansion chamber. Large droplets were generated by Formulation 2 during the early atomization phase, and they remained and moved quickly in front of the main spray (Fig. 1(d)). Formulation 2 has a higher fraction of propellant HFA 134a and generates a higher pressure, which causes the liquid phase of the formulation to be expelled quickly by high pressure without full evaporation. On the contrary, Formulation 1 produces better atomization. Different from a typically linearly spreading turbulent round jet (Pope, 2000), the flashing liquid jet issuing from a circular nozzle, was divided by Yildiz et al. (2002) into an expansion region and an entrainment region. They experimentally observed the jet in the expansion region moving with increasing velocity. The velocity starts to decrease in the entrainment region due to mixing with ambient air as the jet propagates until it reaches its minimum as droplets evaporate. Hence, several parameters are required to be defined to characterize the spray as shown in Fig. 3. Although the cone angle of a spray needs to be measured from the virtual origin of the turbulent jet, the diameter of the discharge orifice (0.2 mm) is small enough to neglect the virtual origin position (Kotsovinos, 1976). All spray angles in this study were measured from the discharge orifice. An unprocessed sample of jet generated under 1st shallow inhalation with Formulation 1 by Oxette® 2 is shown in Fig. 3(a). The spray outline was picked out after an image process with a threshold level of 85% of the background intensity, as shown in Fig. 3(b), where the detailed image process technique can refer to Ju et al. (in press). Morgan et al. (2001) concluded that the measured values were insensitive to the threshold level chosen, but the threshold value has to be constant during processing of the images. The spray penetration was measured by finding the spray pixel furthest from the discharge orifice along the axis. This value of penetration was then used to calculate the half spray angle (θ_3 and θ_4) at half the maximum penetration length. Similarly the half spray angle in the expansion region is defined as θ_1 and θ_2 in Fig. 3(b).

In our experiment, the corresponding jet tip penetrations and penetration rates under 1st shallow inhalation and 1st deep inhalation during 0.001–0.012 s from the start of actuation were measured from the raw data (for example, Fig. 1) and shown in Fig. 4. Under the 1st shallow inhalation, the jet axial velocities followed the trend discovered by the previous researchers (Yildiz et al., 2002; Calay and Holdo, 2008; Polanco et al., 2010), where the peak velocities were detected at 0.002 s for both formulations, which indicated the expansion ended at approximately 30 mm from the discharge orifice (spray front tip position at 0.002 s); Formulation 2 generated a faster jet at a mean velocity of 10.1 m/s

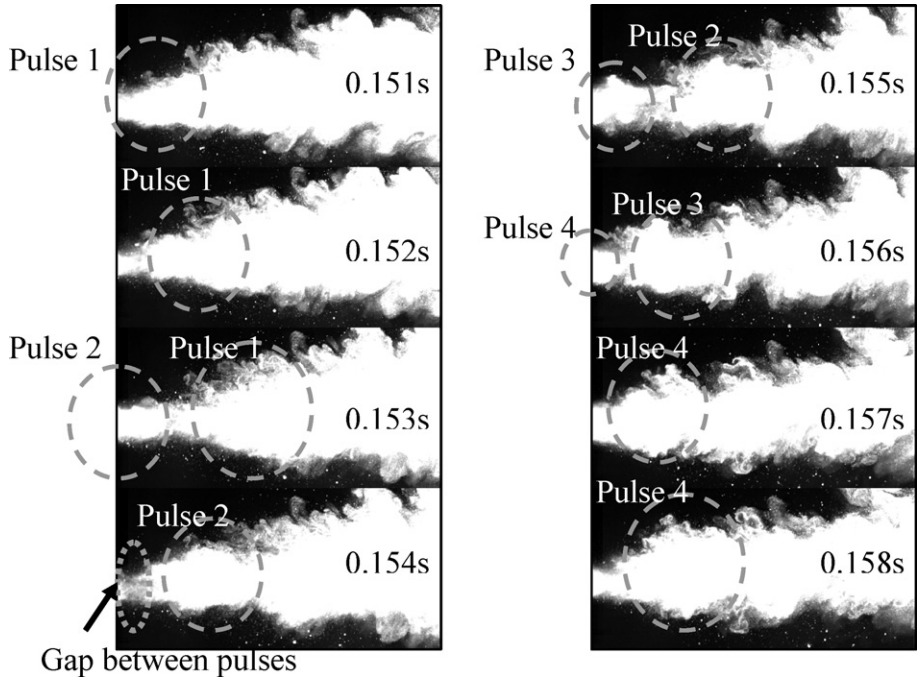

Fig. 6. Spray visualization at the expansion region from 0.151 s to 0.158 s under 1st shallow inhalation with Oxette® 2 for the Formulation 2 (98% HFA 134a). Four pulses were observed with a time interval of 1–2 ms, each pulse caused a large fluctuation of spray cone angle.

compared with 9.4 m/s generated by Formulation 1 under the 1st shallow inhalation. Under the 1st deep inhalation, the maximum velocities were found at 0.001 s around 20 mm from the discharge orifice, which indicates the jet generated by the shallow inhalation has a longer expansion region than that under deep inhalation.

The spreading rate of a turbulent round jet can be defined as Eq. (1) from the half spray angle

$$S = \frac{dr_{1/2}(x)}{dx} = \tan\left(\frac{\theta}{2}\right) \quad (1)$$

where $r_{1/2}$ is the jet's half width, θ is the half spray angle (θ_1 to θ_4 in Fig. 3(b)) and x is the axial length of the jet from the discharge orifice.

Fig. 5 shows the spray development sequences of the jet flow during 0.1–1.1 s under the 1st shallow inhalation for the Formulation 1 and Formulation 2. It is thought the boiling process dominates the spray characters in the expansion region and turbulent mixing dominates during the entrainment region. Formulation 2 has a higher propellant (HFA 134a) mass fraction (98%) than Formulation 1 (95%), so that Formulation 2 evaporated more into the ambient environment at 1.1 s resulting in a sparser spray than that generated by Formulation 1. Vu and Aguilar (2009) suggested that a combination of evaporation and boiling processes can describe the external flow of a flashing jet. The boiling process is a volume based phenomenon, which can be observed from the internal flow (Fig. 2) and external expansion region. Large drops were produced from upper and lower edges of the discharge orifice at the expansion region of the spray generated by Formulation 2, which indicates there is an internal annular flow in the discharge orifice. At the expansion region, the "explosion" phenomena became weak after 0.8 s from the start of the actuation, which is due to the reduction of the formulation actuated and the decrease of the degree of superheat.

The spray cone angles and spreading rates at different time steps were measured under the 1st shallow inhalation by Oxette® 2 for both formulations and listed in Table 1 (Appendix A). Due to the higher vapour pressure of Formulation 2 caused by the higher mass fraction of propellant, Formulation 2 was actuated faster and had a shorter flow duration (1.1 s) than that of Formulation 1 (1.4 s). For both of the formulations, the averaged upper angles are larger (θ_1 and θ_3) than the lower angles (θ_2 and θ_4), which was caused by the entrainment from the vent at the top of the Oxette® (Fig. 3(a)) and the recirculation in the closed inspiration chamber. Compared to Formulation 1, the spray generated by Formulation 2 has higher vapour pressure, which causes the boiling phenomena to be more "violent" and the averaged θ_1 larger than that of Formulation 1. Due to a higher mass fraction of HFA 134a, Formulation 2 evaporated more into the ambient environment resulting in a smaller spray angles (θ_3 and θ_4) than that generated by Formulation 1 in the entrainment region.

Different from the turbulent round jet of a single phase spreading linearly at a constant spreading rate of 0.10 (Pope, 2000), the spreading rates of a flashing jet are unsteady with time. Standard deviations (STD) of the spray angle (θ_1) show the pulsations in the spray produced by Formulation 2 are more notable than those of Formulation 1 in the expansion region. Dunbar (1996) measured the half spray angles of the jet issuing from a pMDI with pure HFA 134a, where the angles were 8.5–11.3° at 0–50 mm from the discharge orifice and 10.2–11.9° at 50–125 mm from the discharge orifice. Dunbar (1996) did not observe the boiling phenomena in the expansion region since it was blocked by the mouthpiece. He found the upper and lower region of the spray were approximately symmetric, which is caused by the different vent designs of the pMDI where the ventilation surrounds the whole jet.

Periodic pulsations can be observed near the discharge orifice and some visualisations of the jet expansion region are shown in Fig. 6, where the photos were taken between 0.151 s and 0.158 s from the start of actuation at a frame rate of 1000 Hz. There are clear gaps between pulses. Each pulsation causes a large fluctuation of the instantaneous spray cone angle. The time scale between two sequential pulses is 1–2 ms.

Domnick and Durst (1995) concluded that the periodic behaviour is the result of the bubble growth process which depends

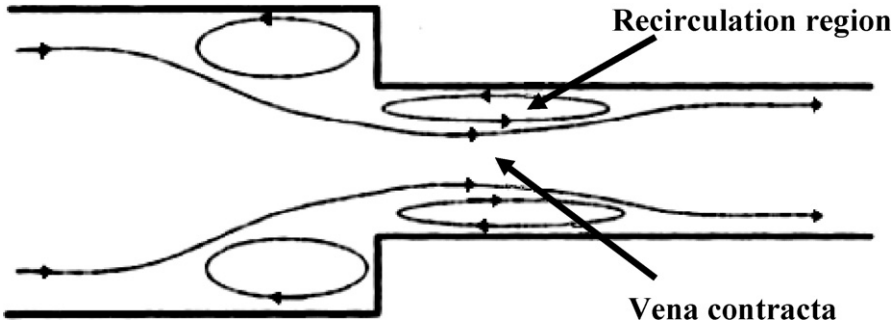

Fig. 7. Mean streamlines of the flow in a constriction examined by Domnick and Durst (1995). Recirculation was observed inside the constriction where bubbles grew and expanded.

on the evaporation process and the location of bubble creation. They tested the flow and showed that bubble growth occurs in recirculation regions inside the constriction (Fig. 7). The lowest pressure in this flow occurs in the cross-section where the recirculation regions and vena contracta are present. Nucleation bubbles that enter the recirculation region are exposed to this reduced pressure for a longer time than bubbles that stream through and which are not captured by the recirculation region. The increased residence time of bubbles in the recirculation region allows such bubbles to undergo large growth, causing the volume of the recirculation region to grow until it obstructs enough of the channel that the incoming liquid flushes a large portion of the recirculation region downstream. Bubbles in the recirculation region, which are reduced in size after this flushing, then build up the size of the recirculation region, and the cycle occurs again. The result is a rapidly oscillating/periodic bubbly flow downstream at a frequency of 500–800 Hz (Domnick and Durst, 1995).

Fig. 8 provides a closer view on the expansion region of the jet which was recorded at the frame rate of 5 kHz. Fig. 8(a) shows a new pulse (pulse 2) pushed out from the discharge orifice and pulse 1 dispersed into atmosphere in Fig. 8(b). Another new pulse (pulse 3) formed in Fig. 8(d). There is a 0.6 ms time interval between pulse 2 and pulse 3, which is smaller than that discovered by Domnick and Durst (1995) and Dunbar (1996). It implies the pulsation of the jet is unsteady with time and it remains complex to analyse.

3.2. Drop sizing at an axial distance of x = 100 mm from the discharge orifice

Drop sizing work is done at the position of (100 mm, 0 mm) from the discharge orifice by our newly developed particle/droplet image analysis (PDIA) method (Ju et al., in press), illustrated using a high speed laser system. The droplet information was recorded during 0–2 s of the actuation with 500 Hz camera exposure frequency under the 1st shallow inhalation. The number distribution of the droplets is shown in Fig. 9 for Formulation 1 (95% HFA 134a) and Formulation 2 (98% HFA 134a). Both formulations generated a peak at 8–10 μm. Due to the smaller mass fraction of inerts of Formulation 2, a larger number of droplets with diameter smaller than 10 μm were formed by Formulation 2. The oscillations in the figures are caused by the occasional large droplets generated by the ligaments as show in Fig. 10.

Mean diameters D_{10} (Eq. (2)), $D_{0.1}$, $D_{0.5}$ and $D_{0.9}$ are used to compared the drop sizes at different time scales and the results are presented in Table 2 (Appendix A), where the droplet information was acquired from 1000 images every 0.2 s time interval. The smallest mean diameters and most dense spray (according to the

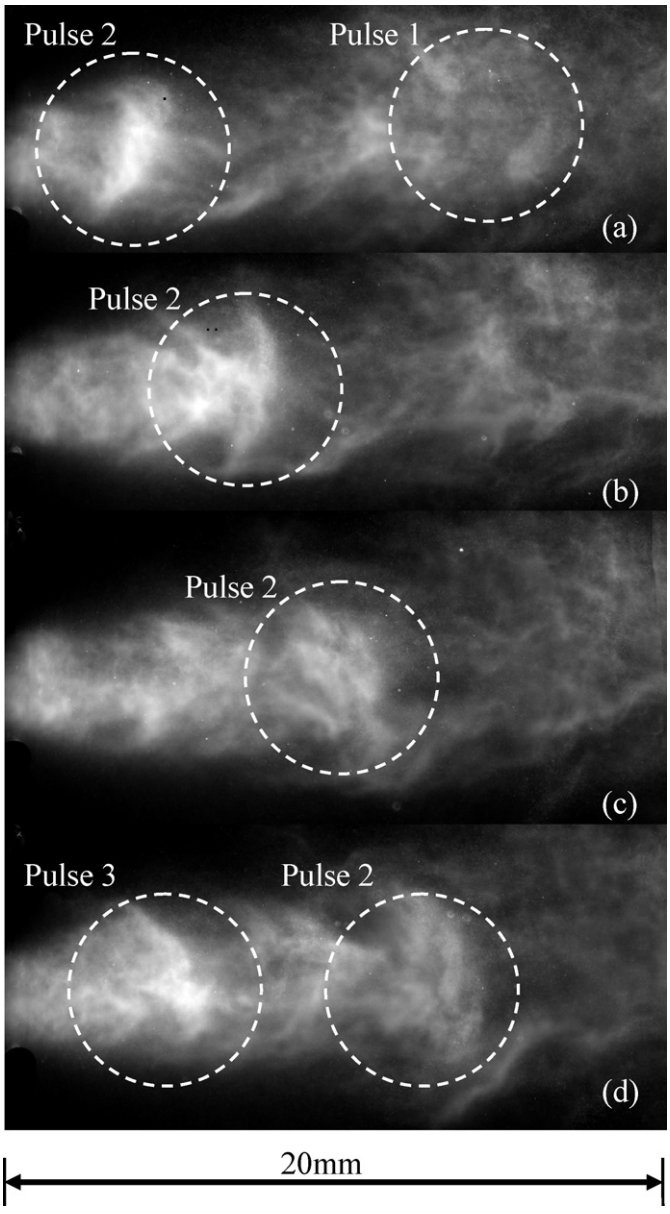

Fig. 8. Close visualizations on the pulsations near the exit of the discharge orifice (sequentially recorded at 5 kHz).

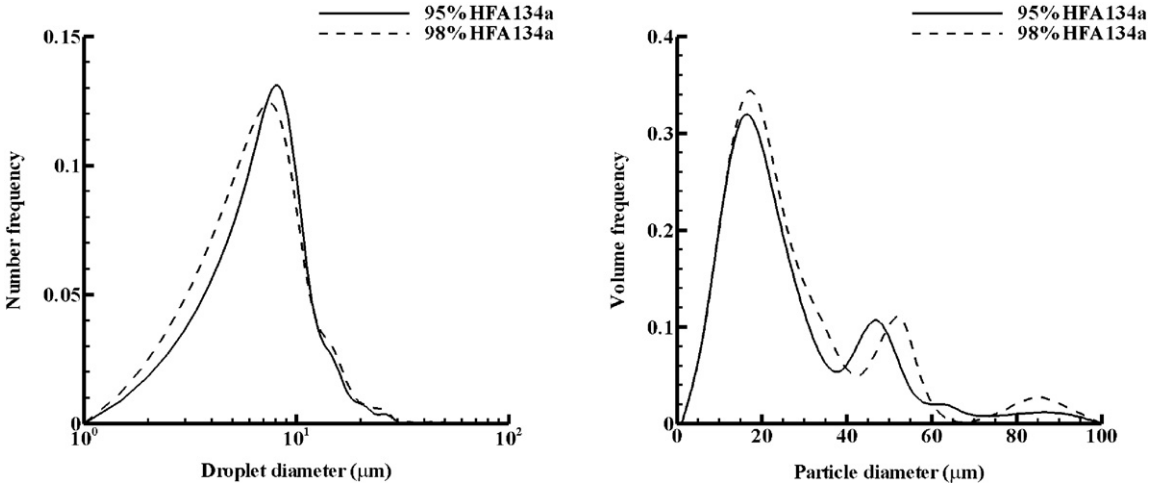

Fig. 9. Number and volume based size distributions of the droplets for the spray generated by Formulation 1 (95% HFA 134a) and Formulation 2 (98% HFA 134a) under the 1st shallow inhalation.

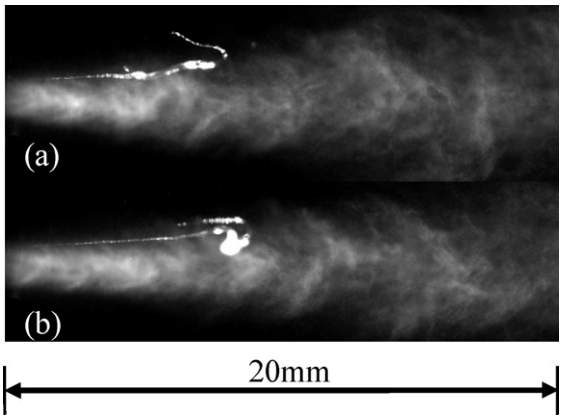

Fig. 10. (a) A ligament was generated occasionally from the actuation. (b) A large drop was formed by the ligament in (a).

detected droplet number) are detected at 0.4–0.6 where the inhalation pressure is minimum and the convection effect is maximum.

$$D_{10} = \frac{\sum N_i D_i}{\sum N_i} \quad (2)$$

Mean diameters were acquired under 1st shallow inhalation with Oxette® 2 for the Formulation 1 and Formulation 2. Ten tests were operated under the same conditions for each formulation and results are shown in Table 3 (Appendix A). 1000 images were analyzed for each test. According to the droplet number detected, more than twice the droplet number was detected for Formulation 1 than that for Formulation 2, which is due to its higher mass fraction of inerts and droplets with diameters smaller than 3 μm may be lost due to the calibration threshold of the system (Ju et al., in press).

Clark (1991) measured the initial MMD of the spray produced by a pMDI near the exit is 12.5–22.5 μm for the formulation with 98% mass fraction of HFA 134a and 2% PEG300. Similarly Dunbar (1996) measured residual $D_{0.1}$ and $D_{0.3}$ of the spray issued from a pMDI at x = 100 mm are 2.6 μm and 4.5 μm with pure HFA 134a. Their results are sensibly smaller than our measurement. The difference is caused by the smaller expansion chamber volume of the Oxette® and the in-line geometry of expansion chamber in the Oxette® provides less chance for the recirculation to form bubbles. Our numerical model from the first paper (Ju et al., 2012) predicted the residual MMD at x = 100 m is 8–13 μm, which again under-estimated the droplet sizes compared to our imaging results. The occasional large droplets as shown in Fig. 10 increased the

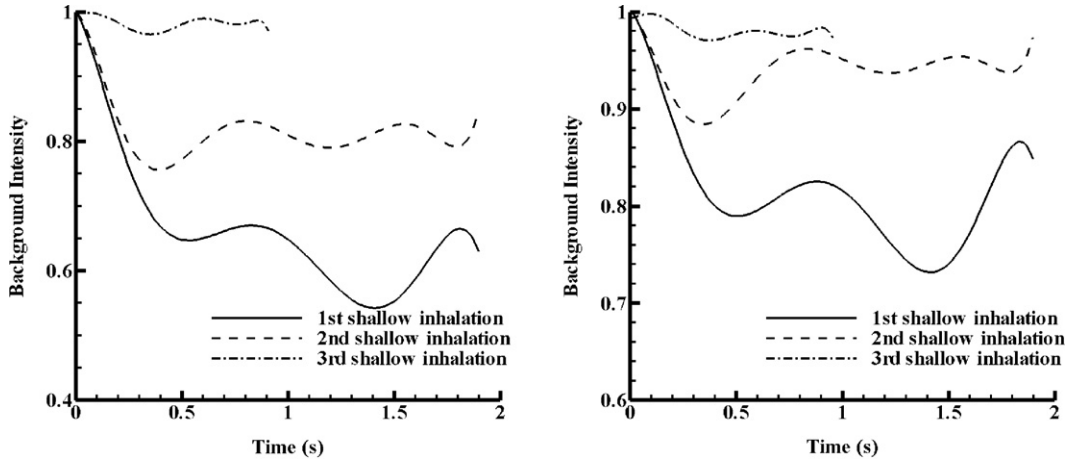

Fig. 11. The background intensity variations of the droplet images (by the direct imaging method) for the spray generated by Oxette® 2 with Formulation 1 (left: 95% HFA 134a) and Formulation 2 (right: 98% HFA 134a) under 1st, 2nd and 3rd shallow inhalation at x = 100 mm. The variations agree with equivalent measurement by the dual laser method in the first paper (Ju et al., 2012).

residual MMD in sizing the droplets. Furthermore, the limitations of our imaging system (Ju et al., in press) will be unable to detect the droplets of a diameter smaller than 3 μm due to its calibration threshold.

Fig. 11 shows the background intensity variations of the droplet images, which correlates with the plume opacity, for the spray generated by Oxette® 2 at $x = 100$ mm from the discharge orifice with two formulations under sequentially shallow inhalations. The plume opacity of the spray generated by Formulation 1 is twice of that of Formulation 2 during the 1st and 2nd shallow inhalations, because Formulation 2 has a higher mass fraction of HFA 134a leading to a faster evaporation rate, and it produced sparser sprays at $x = 100$ mm compared to Formulation 1. It agrees with the dual laser measurement of the first paper (Ju et al., 2012). The relative densities of the spray are inversely proportional to the background intensities of the droplet images. For Formulation 1, the ratio of the averaged density of the spray generated under the 1st and 2nd shallow inhalation is 0.71, while the ratio is 0.57 for Formulation 2. It indicates Formulation 1 produces more steady spray than Formulation 2. However, it performs differently from a pMDI (Ju et al., 2010), since the pMDIs were tested in an open environment while the Oxette® was tested in a closed observation chamber. The spray issued from a pMDI dispersed into atmosphere after the end of the actuation, which is not detectable by the dual laser method. However, the sprays generated by Oxette® were measured in a closed chamber where droplets settled, and recirculated inside the chamber and were detectable by the dual laser method after the inhalation. The pulsations of the curves after 1.0 s from the actuation, shown in Fig. 11, were caused by the recirculation of the flow during the exhalation condition.

4. Conclusion

Two different formulations with 95% and 98% mass fraction of HFA 134a and two early stage prototypes of cigarette alternatives with different expansion chamber volumes have been analyzed by high speed imaging system. The internal and external flows issuing from the "Oxette®" devices were visualized and discussed along with the boiling and evaporating phenomena. Furthermore, droplet sizes were measured by our newly developed imaging system (Ju et al., in press) at the distance from the discharge orifice where the human oropharynx locates. Although Formulation 2 (98% HFA 134a) can generate smaller droplets, Formulation 1 (95% HFA 134a) produces more steady puffs with relatively low mass flow rate. From the visualization of the internal flow in the earlier prototype (Oxette® 1), small expansion chambers can hardly generate small bubbles to produce fine sprays. The later design (Oxette® 2) significantly improves the performance and produces finer sprays, due to its larger the expansion chamber volume for the propellant evaporation, recirculation, bubble generation and growth. Compared to the pMDI, the Oxette® has a smaller expansion chamber and the geometry provides less opportunity for the recirculation to form the small bubbles, which causes the residual MMD near the oropharynx to be larger than that of a pMDI.

Acknowledgements

We appreciated the technical support from Simon R. Klitz, and funding and prototypes supplement from Kind Consumer Ltd. (http://www.kindconsumer.com/).

Appendix A.

Tables 1–3.

Table 1
Half spray cone angles and spreading rates under 1st shallow inhalation with Oxette® 2 for the formula Formulation 1 (95% HFA 134a) and Formulation 2 (98% HFA 134a) from 0.1 s to 1.4 s.

Time step	Half spray angle (°)				Spray spreading rate			
	θ_1	θ_2	θ_3	θ_4	S_1	S_2	S_3	S_4
Formulation 1								
0.1	16	8	14	6	0.11	0.06	0.10	0.04
0.2	15	13	12	8	0.10	0.09	0.08	0.05
0.3	18	10	12	6	0.12	0.07	0.09	0.04
0.4	14	10	13	9	0.10	0.07	0.09	0.06
0.5	16	10	12	8	0.11	0.07	0.08	0.06
0.6	15	10	13	8	0.10	0.07	0.09	0.06
0.7	14	8	14	7	0.09	0.06	0.10	0.05
0.8	16	10	18	9	0.11	0.07	0.12	0.06
0.9	16	10	18	10	0.11	0.07	0.13	0.07
1.0	22	13	18	11	0.15	0.09	0.12	0.07
1.1	16	12	17	13	0.11	0.08	0.12	0.09
1.2	14	10	16	11	0.09	0.07	0.11	0.07
1.3	12	11	15	12	0.08	0.08	0.10	0.08
1.4	11	10	15	11	0.08	0.07	0.10	0.08
Average	15	10	15	9	0.11	0.07	0.10	0.06
STD	1.4	1.7	0.9	1.0	0.02	0.01	0.02	0.01
Formulation 2								
0.1	16	9	12	7	0.11	0.06	0.08	0.05
0.2	15	12	10	6	0.11	0.08	0.07	0.04
0.3	15	9	13	8	0.10	0.06	0.09	0.05
0.4	17	7	13	7	0.12	0.05	0.09	0.04
0.5	20	7	13	8	0.14	0.05	0.09	0.05
0.6	18	7	17	6	0.12	0.05	0.11	0.04
0.7	20	13	15	7	0.14	0.09	0.10	0.05
0.8	14	6	18	5	0.10	0.04	0.13	0.04
0.9	13	7	14	6	0.09	0.05	0.10	0.04
1.0	13	5	12	5	0.09	0.03	0.08	0.04
1.1	13	5	12	5	0.09	0.03	0.08	0.04
Average	16	8	14	6	0.11	0.06	0.09	0.04
STD	2.0	2.4	2.0	0.7	0.02	0.02	0.02	0.01

Table 2
Mean diameters (μm) at different time scales under 1st shallow inhalation with Oxette® 2 for the Formulation 1 (95% HFA 134a) and Formulation 2 (98% HFA 134a). $D_{0.1}$: drop diameter such that 10% of total liquid volume is in drops of smaller diameter. $D_{0.5}$: drop diameter such that 50% of total liquid volume is in drops of smaller diameter, which is the mass median diameter (MMD). $D_{0.9}$: drop diameter such that 90% of total liquid volume is in drops of smaller diameter.

Time scale (s)	D_{10}	D_{32}	$D_{0.1}$	$D_{0.5}$	$D_{0.9}$	$D_{0.5}/D_{32}$	Detected droplet number
Mean diameters (μm) for Formulation 1							
0–0.2	16.8	24.7	12.8	25.3	44.8	1.02	12
0.2–0.4	9.8	20.1	10.3	25.3	56.3	1.25	3921
0.4–0.6	9.8	17.1	9.3	19.8	46.8	1.15	3527
0.6–0.8	10.3	18.4	10.3	21.3	51.3	1.15	2763
0.8–1.0	10.4	19.2	10.3	24.3	50.3	1.26	2014
1.0–1.2	11.0	21.4	11.8	25.8	66.8	1.21	1787
1.2–1.4	10.8	21.4	12.8	26.3	49.3	1.23	1907
1.4–1.6	10.3	21.0	12.8	25.8	51.3	1.23	1676
1.6–1.8	10.3	20.6	11.8	25.3	55.8	1.23	1513
1.8–2.0	10.1	18.9	10.3	23.3	49.3	1.23	1230
Average	10.9	20.3	11.2	24.2	52.2	1.20	2035
Mean diameters (μm) for Formulation 2							
0–0.2							0
0.2–0.4	9.3	18.0	9.3	21.3	53.3	1.18	1331
0.4–0.6	9.0	16.0	8.8	17.8	54.3	1.11	1563
0.6–0.8	10.1	18.2	9.3	21.3	61.8	1.17	1326
0.8–1.0	10.1	18.5	9.8	22.3	62.3	1.21	982
1.0–1.2	9.3	16.8	8.8	19.3	54.3	1.14	711
1.2–1.4	9.7	17.0	8.8	19.8	50.8	1.16	577
1.4–1.6	9.9	17.9	9.3	18.3	38.8	1.19	416
1.6–1.8	10.2	16.1	9.3	18.3	38.8	1.14	392
1.8–2.0	10.6	19.2	10.3	22.3	70.8	1.16	362
Average	9.8	17.5	9.3	20.0	53.9	1.16	766

Table 3
Mean diameters (μm) at each test under 1st shallow inhalation with Oxette® 2 for the Formulation 1 (95% HFA 134a) and Formulation 2 (98% HFA 134a).

Test index	D_{10}	D_{32}	$D_{0.1}$	$D_{0.5}$	$D_{0.9}$	$D_{0.5}/D_{32}$	Detected droplet number
Mean diameters (μm) for Formulation 1							
1	9.7	18.1	9.8	21.3	49.3	1.18	2387
2	9.6	19.7	10.3	24.3	62.8	1.23	2284
3	9.7	18.2	9.8	21.3	51.3	1.17	2244
4	9.7	17.8	9.8	21.3	47.3	1.20	2258
5	9.6	18.7	10.3	23.3	53.3	1.24	1856
6	10.5	19.4	10.8	26.8	65.8	1.18	1964
7	10.8	20.1	11.3	24.3	51.3	1.21	2331
8	10.8	22.5	12.8	26.8	65.8	1.19	1891
9	11.0	20.1	11.3	24.3	49.3	1.21	1485
10	10.9	21.5	12.3	26.3	59.8	1.22	1647
Average	10.2	19.6	10.8	24.0	55.6	1.20	2035
Mean diameters (μm) for Formulation 2							
1	9.9	18.8	10.3	22.8	51.3	1.21	1118
2	9.6	16.6	8.8	19.3	55.3	1.16	837
3	9.1	15.3	8.3	17.3	45.3	1.13	907
4	9.5	18.3	9.3	22.8	72.8	1.24	614
5	9.9	16.8	9.3	19.3	52.8	1.14	740
6	9.2	17.0	9.3	19.8	50.8	1.16	607
7	9.9	17.4	9.8	20.3	47.8	1.16	750
8	9.9	18.3	9.8	21.3	61.8	1.16	712
9	9.6	17.8	9.3	20.8	57.8	1.16	783
10	9.5	18.0	9.3	20.8	70.8	1.16	634
Average	9.6	17.4	9.3	20.4	56.6	1.17	770

References

Calay, R.K., Holdo, A.E., 2008. Modeling the dispersion of flashing jets using CFD. J. Hazard. Mater. 154, 1198–1209.

Clark, A.R., 1991. Metered atomization for respiratory drug delivery. Ph.D. thesis. Loughborough University of Technology, UK.

Domnick, J., Durst, F., 1995. Measurement of bubble size, velocity and concentration in flashing flow behind a sudden constriction. Int. J. Multiphase Flow 21, 1047–1062.

Dunbar, C.A., 1996. An experimental and the theoretical investigation of the spray issued from a pressurized metered-dose inhaler. Ph.D. thesis. Institute of Science and Technology, University of Manchester.

Ju, D., Shrimpton, J., Hearn, A., 2010. The effect of reduction of propellant mass fraction on the injection profile of metered dose inhalers. Int. J. Pharm. 391, 221–229.

Ju, D., Shrimpton, J., Hearn A. A multi-thresholding algorithm for sizing out of focus particles. Part. Part. Syst. Charact., in press.

Ju, D., Shrimpton, J., Bowdrey, M., Hearn, A., 2012. Effect of expansion chamber geometry on atomization and spray dispersion characters of a flashing mixture containing inerts. Part I. Numerical predictions and dual laser measurements. Int. J. Pharm., http://dx.doi.org/10.1016/j.ijpharm.2012.04.065.

Kotsovinos, N.E., 1976. A note on the spreading rate and virtual origin of a plane turbulent jet. J. Fluid Mech. 77, 305–311.

Morgan, R., Wray, J., Kennaird, D.A., Crua, C., Heikal, M.R., 2001. The Influence of Injector Parameters on the Formation and Break-Up of a Diesel Spray. Society of Automotive Engineers, Inc, 2001-01-0529.

Polanco, G., Holdo, A.E., Munday, G., 2010. General review of flashing jet studies. J. Hazard. Mater. 173, 2–18.

Pope, S.B., 2000. Turbulent Flows. Cambridge University Press, Cambridge, UK.

Versteeg, H.K., Hargrave, G.K., Kirby, M., 2006. Internal flow and near-orifice spray visualisations of a model pharmaceutical pressurised metered dose inhaler. J. Phys.: Conf. Ser. 45, 207–213.

Vu, H., Aguilar, G., 2009. High-speed internal nozzle flow visualization of flashing jets. In: ICLASS 2009, 11th Triennial International Annual Conference on Liquid Atomization and Spray Systems, Vail, CO, USA, July 2009.

Yildiz, D., Rambaud, P., Vanbeeck, J., Buchlin, J.M., 2002. A study on the dynamics of a flashing jet. Final contract research report EAR0030/2002. von Karman Institute for Fluid Dynamics.